Thin-film superparamagnetic resonance in a γ-Fe_2O_3 nanoparticle array

S. Zohar,[a] K. Hultman, S. O'Brien, and W. E. Bailey[b]
Materials Science Program, Department of Applied Physics and Applied Mathematics, Columbia University, 500 W 120th St., New York, New York 10027, USA

(Presented on 8 November 2007; received 5 September 2007; accepted 3 October 2007; published online 23 January 2008)

We have investigated the microwave properties of monodisperse, superparamagnetic γ-Fe_2O_3 nanoparticle arrays using broadband ferromagnetic resonance. We identify a novel field for resonance relationship in the films. Compared with ferromagnetic films of equal magnetization, resonance frequencies are suppressed for in-plane magnetization and enhanced for out-of-plane magnetization, over the range of 0–8 Ghz. The behavior identified is that of a superparamagnetic thin film, where thin-film dipolar fields act on a gradually saturating magnetization described by the Langevin function. Resonance linewidths can be described by the natural thermal dispersion in properties of the system. © *2008 American Institute of Physics*. [DOI: 10.1063/1.2829392]

Self-assembled nanocrystal (NC) arrays, ordered in two[1] or three dimensions,[2] offer new opportunities for controlled properties in functional materials. The control of optoelectronic properties of semiconductor NCs, through monodisperse size[3] ($\pm 10\%$ rms typical) and regular spacing[4] is well established. In magnetic NC systems, such as ferrimagnetic γ-Fe_2O_3, size controls the stability of ferromagnetism (FM) and superparamagnetism (SP),[5] and spacing can control exchange or dipolar interactions between particles.[6] Monodisperse magnetic NCs and NC assemblies have many applications prospects: noninteracting SP NCs for contrast enhancement agents in NMR,[7,8] weakly interacting FM two-dimensional (2D) arrays for magnetic storage media with improved thermal stability,[9] and strongly interacting FM three-dimensional (3D) arrays for permanent magnets with improved energy products.[10]

SP NC films have been proposed as candidate microwave passive materials at frequencies $\omega/2\pi > 1$ Ghz.[11] Compared with ferromagnetic thin films, SP NC arrays offer some greater flexibility in conformal processing and in setting the net ferromagnetic resonance (FMR) frequency ω_{res} through layered composites. A critical question is what determines ω_{res} in a SP NC array. For ferromagnetic or ferrimagnetic films, the dominant role of shape anisotropy in ω_{res} is widely recognized:[12,13] the effective field is set primarily through the magnetic moment $4\pi M_s$, fixed in magnitude. The role of shape in magnetic resonance of superparamagnetic NC films or arrays has not yet been recognized. Fixed-frequency studies on monodisperse Co NC arrays[14] or γ-Fe_2O_3 suspensions[15] have been interpreted in terms of variable anisotropy, neglecting any influence of shape.[16] Variable-frequency studies on ferromagnetic (23 nm) NC compacts have been carried out in bulklike compacts where shape effects are absent.[17]

In this paper, we show that the resonant frequencies of monodisperse, SP NC arrays can be interpreted simply. The Kittel expressions for thin-film FMR, which take shape effects into account, can be modified to incorporate the variable magnetization $M=M(H)$ according to the paramagnetic Langevin function. Good agreement is found between a parameter-free model and experimental FMR frequencies with in-plane magnetization $\omega_{\|}$ and out-of-plane magnetization $\omega_{\perp}$.

Spherical, monodisperse 7.5 nm diameter γ-Fe_2O_3 nanoparticles were synthesized according to the method described in Refs. 18 and 19 and dissolved in hexane. A drop of the solution was placed onto a transmission electron microscopy (TEM) Si_3N_4 membrane and allowed to dry; the corresponding 200 keV TEM image is shown in Fig. 1. Samples for FMR measurement were prepared similarly on GaAs substrates, but thicker films (~20 drops or ~20–40 monolayers) were necessary to observe a strong FMR signal. Analysis of the TEM image using a cluster labeling algorithm[20] yields an average particle center-to-center spacing of 10.5 nm. Of the 3 nm gap between particle edges, the ligands contribute ~1 nm per particle and ~1 nm results from imperfect packing. In a 3D array, we estimate a volume packing reduced by

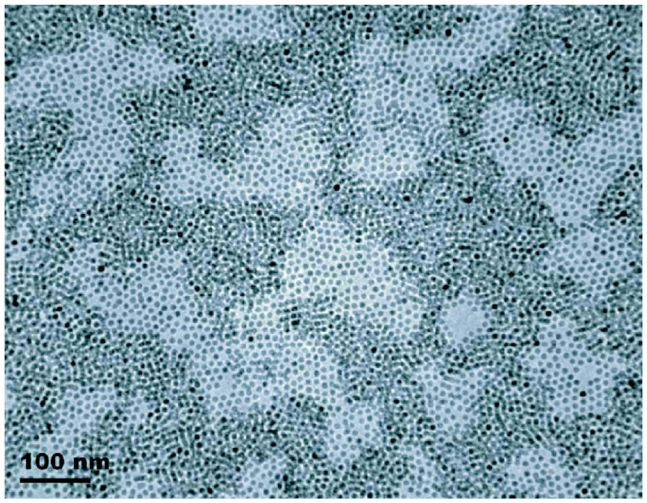

FIG. 1. (Color online) TEM image of 1–2 monolayers of 7.5 ± 0.8 nm γ-Fe_2O_3 nanoparticles. Light and dark regions correspond to single- and double-monolayer regions, respectively. Local hexagonal ordering is clearly seen; an average center-to-center spacing of 10.5 nm is identified in one-monolayer regions.

[a]Electronic mail: sz2123@columbia.edu.
[b]Electronic mail: web54@columbia.edu.

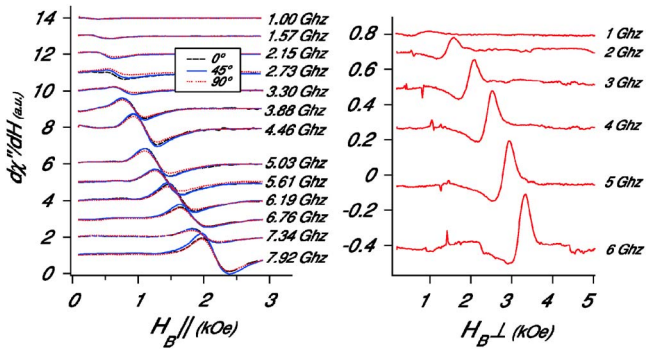

FIG. 2. (Color online) Broadband FMR measurements of 7.5 nm SP γ-Fe_2O_3 thin film. Left: pc measurements of $\omega_\parallel$, for field H_B orientations of 0, 45, and 90° to sample flat. Right: nc measurements of $\omega_\perp$. See text for details.

a factor of $(7.5/10.5)^3 \simeq 0.36$ from a close packed structure, or a packing fraction of 0.27.

We have characterized the films using broadband FMR, over a frequency range of 0–8 Ghz, at room temperature. Films were inverted and placed on a coplanar waveguide (CPW) fabricated on GaAs. Absorption spectra were taken over a series of fixed frequencies using field-swept, field-modulated measurements, as described in Ref. 21. Measurements were taken in the parallel configuration (pc), with applied fields H_B in the film plane, and normal configuration (nc), with applied fields H_B normal to the film plane, to measure $\omega_\parallel$ and $\omega_\perp$, respectively.

FMR spectra are shown in Fig. 2 for a series of discrete frequencies. Symmetric spectra are observed with single absorption lines, characteristic of superparamagnetic particles.[16] Line strengths increase with increasing frequency (field); fields for resonance $H_{\rm res}$ increase with frequency, yielding increasing $\omega_\parallel(H_B)$ and $\omega_\perp(H_B)$. half power linewidths ΔH are on the order of 200–500 Oe, increasing with frequency.

Experimental $\omega_\parallel(H_B)$ and $\omega_\perp(H_B)$ are summarized in Figs. 3 and 4. In the top panel, we compare the measured values with calculations based on the Kittel equations for thin-film FMR, $\omega_\parallel = \gamma\sqrt{(H_B+H_K+4\pi M_s)(H_B+H_K)}$ and $\omega_\perp = \gamma(H_B-4\pi M_s)$, where γ is the gyromagnetic ratio $\gamma = e/2m_{\rm eff}c \simeq 17.588$ Mhz/Oe$(g_{\rm eff}/2)$, and H_K is the effective field from anisotropy. According to the independence of $\omega_\parallel$ on the in-plane rotational angle (0, 45°, 90°), the average H_K is taken to be zero. Using the TEM micrograph estimate of the packing fraction for the (3D) film of 0.27, with the known saturation magnetization of maghemite $4\pi M_s = 5.35$ kG,[22] we estimate the effective, saturated $4\pi M_s$ of our nanoparticle film as 1.5 kG. Using these *fixed* values of $4\pi M_s$ (Kittel model) significantly *underestimates* the nc resonance frequency $\omega_\perp$ and *overestimates* the pc resonance frequency $\omega_\parallel$, compared with the experimental values, at low fields and frequencies. At higher fields and frequencies, data and the Kittel resonances begin to converge.

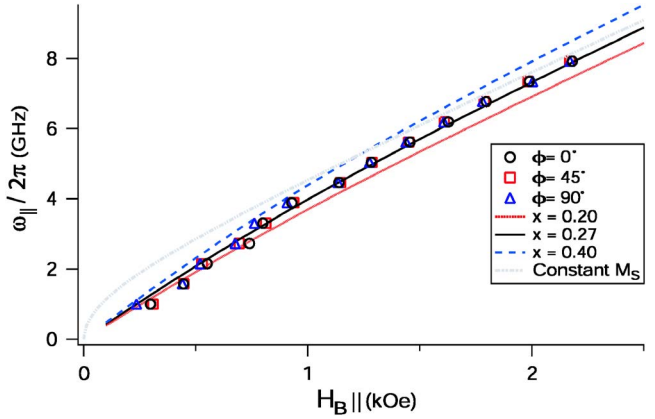

FIG. 3. (Color online) Resonance frequencies $\omega_\parallel(H_B)$, for different field orientations ϕ, in-plane (pc) configuration, from Fig. 2, left. Model calculations for thin-film superparamagnetic resonance [Eq. (1)], varying volume fraction x from TEM-measured $x=0.27$. See text for details.

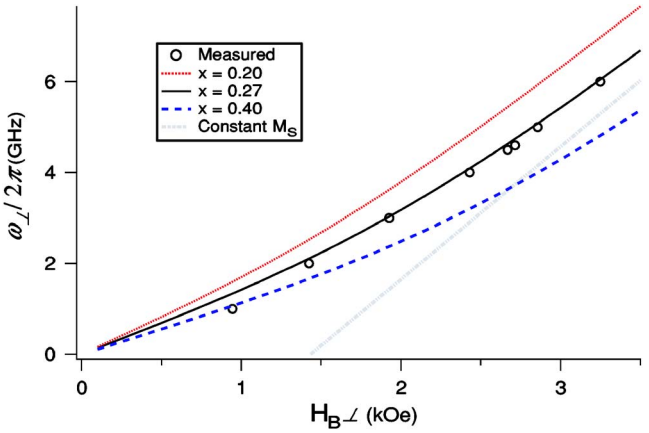

FIG. 4. (Color online) Resonance frequencies $\omega_\perp(H_B)$ for normal configuration (nc), calculated according to Eq. (1), as in Fig. 2.

We propose a model which takes into account the sizeable unsaturated moment M of the thin-film superparamagnetic assembly. As the spherical particle with diameter D has a total moment $\mu = \pi M_s D^3/6$, our maghemite particles with $D=7.5$ nm have a total moment of $\sim 6\times 10^4 \mu_B$, well into the classical (Langevin) limit for paramagnetism. The saturation behavior of the particle can then be described by the Langevin function[23] $M(H)/M_s = \mathfrak{L}(s) = \coth s - 1/s$, $s = \mu H'/k_B T$, where H' is the local field acting on the nanoparticle. Previous superconducting quantum interference device (SQUID) measurements of similarly prepared γ-Fe_2O_3 7 nm (Ref. 18) and 6–7 nm (Ref. 15) nanoparticles have shown superparamagnetism at room temperature, consistent with our description. For reference, the room-temperature magnetization of a particle of this size will be 50% saturated at local fields ~800 Oe and 90% saturated at ~4400 Oe. We approximate the assembly as a uniformly magnetized thin film lying in the xy plane, where the demagnetizing field $\mathbf{H_d}(\mathbf{r}) = \tilde{\mathbf{N}}\cdot\mathbf{M}(\mathbf{r})$ can be approximated as $\mathbf{H_d} = -4\pi M_z \hat{z}$, so $\mathbf{H'} = \mathbf{H_B} - 4\pi M_z \hat{z}$.

For parallel magnetization (pc), the local field is given simply by $H' = H_B$, and the Kittel relation becomes

$$\omega(H_B) = \gamma\sqrt{\left[H_B + 4\pi M_s \mathfrak{L}\left(\frac{\mu H_B}{k_B T}\right)\right] H_B}, \qquad (1)$$

an explicit function of H_B. For normal magnetization (nc), the local field $H' = H_B - 4\pi M$ can be found only numerically, and the resonance frequency $\omega_\perp = \gamma H'$ is a transcendental function of H_B,

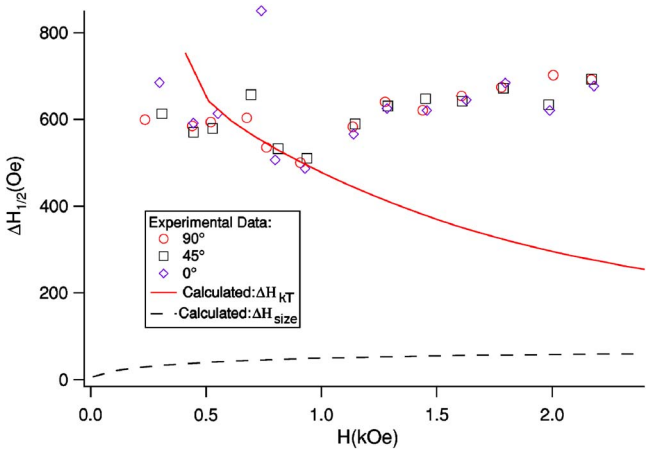

FIG. 5. (Color online) Swept-field peak-to-peak linewidths $\Delta H_{pp}(\omega)$ for the pc resonance data in Fig. 2, left. The calculated effects of 10% dispersions in SP NC size $\Delta H_{size}(\omega)$ and coverage $\Delta H_x(\omega)$ are indicated with anisotropy field dispersion ΔH_K. See text for details.

$$\frac{\omega_\perp(H_B)}{\gamma} = H_B - 4\pi M_s \mathcal{L}\left[\frac{\mu}{k_B T}\frac{\omega_\perp(H_B)}{\gamma}\right]. \quad (2)$$

In applying this model to γ-Fe_2O_3, we have used the nominal $4\pi M_s$ scaled by the packing fraction x, and γ according to the previously measured $g_{\text{eff}}=2.08$.[17] Comparison of the model to experimental data, using the TEM-measured $x=0.27$, shows excellent agreement without free parameter adjustment. The influence of ~10% variations in the packing fraction (to $x=0.2$ and $x=0.4$) is shown. Agreement at fields <500 Oe is somewhat poorer; the influence of noncollinear alignment of moment clusters is possible.[6]

The pc linewidths as a function of frequency $\Delta H(\omega)$ are summarized in Fig. 5. Linewidths have a frequency-independent portion of ~500 Oe and rise by ~100 Oe over the 2–8 Ghz frequency range. In ferromagnetic metals with relatively low loss at low frequency, variable-frequency FMR measurements can be used to separate homogeneous (intrinsic) and inhomogeneous (extrinsic) dampings through the relation $\Delta H(\omega)=2\alpha\omega/\sqrt{3}\gamma$.[24] In the SP NC array, frequency-dependent inhomogeneous broadening mechanisms are likely to be dominant, as the effect of exchange, which averages inhomogeneities in continuous films, is absent.[25]

We calculate and show in Fig. 5 the effects of inhomogeneity on the frequency-dependent half power linewidth $\Delta H_{1/2}(\omega)$. The effects of the upper bound of 10% variation in particle diameter are shown in $\Delta H_{\text{size}}(\omega)$, where the field-swept linewidths ΔH_{size} have been calculated numerically by $(\omega_+ - \omega_-)/(\partial\omega(H)/\partial H)$, and $\omega_{+,-}$ denote the evaluations of ω_{res} at ±10% of the known particle size at ($D=6.3$ and 7.7 nm). We also show the effects of purely thermal dispersion in resonance for monodisperse particle size, calculating a fluctuation in magnetization $\Delta M_{kT}=(\langle M^2\rangle-\langle M\rangle^2)^{1/2}=M_s(1+1/s^2-\coth^2 s)^{1/2}$ from Boltzmann statistics. The magnetization is converted into a standard deviation in resonance field as above, resulting in half power linewidths as shown.[26]

Of the two broadening mechanisms considered, arising either from particle size variations or thermal fluctuations, we find that thermal fluctuations make a substantially larger contribution to the linewidth. Experimental linewidths at low frequency are in reasonable agreement with a purely thermal origin. We note, however, that the observed linewidths are also on the order of known anisotropy fields in γ-Fe_2O_3 ($2K/M_s=1.2$ kG),[27] which will fluctuate from particle to particle due to the random crystal orientation yielding a frequency-independent linewidth; we thus cannot claim that any fit with experiment is unique. At higher frequencies, the intrinsic damping α will be much more important. Intrinsic damping is likely the source of the increasing linewidth with increasing frequency. More quantitative estimates of intrinsic and anisotropic contributions will require measurements at higher frequencies and on oriented ensembles, respectively.

In conclusion, we have shown that magnetic resonance of self-assembled NC arrays can differ strongly from that known in isolated particles or continuous films. Resonant frequencies of superparamagnetic NC arrays are set by a sizeable and variable moment magnitude. Dispersion in particle size and thermal fluctuation of moments leads to resonance broadening in the array larger than would be present in a film of the same composition. The results have implications for gigahertz passive applications of this emerging class of functional materials.

This work has been supported primarily by the MRSEC program of the National Science Foundation under NSF-DMR-0213574.

[1] B. Dabbousi, C. Murray, M. Rubner, and M. Bawendi, Chem. Mater. **6**, 216 (1994).
[2] C. Murray, C. Kagan, and M. Bawendi, Science **270**, 1335 (1995).
[3] L. Brus, Appl. Phys. A: Solids Surf. **A53**, 465 (1991).
[4] C. R. Kagan, C. B. Murray, M. Nirmal, and M. G. Bawendi, Phys. Rev. Lett. **76**, 1517 (1996).
[5] G. A. Held, G. Grinstein, H. Doyle, S. Sun, and C. B. Murray, Phys. Rev. B **64**, 012408 (2001).
[6] M. Kayali and W. Saslow, Phys. Rev. B **70**, 174404 (2004).
[7] M. Olsson, B. Persson, L. Salford, and U. Schroder, Magn. Reson. Imaging **4**, 437 (1986).
[8] J. Bulte and D. Kraitchman, NMR Biomed. **17**, 484 (2004).
[9] S. Sun, C. Murray, D. Weller, L. Folks, and A. Moser, Science **287**, 1989 (2000).
[10] H. Zeng, J. Li, J. Liu, Z. Wang, and S. Sun, Nature (London) **420**, 395 (2002).
[11] V. B. Bregar, IEEE Trans. Magn. **40**, 1679 (2004).
[12] C. Kittel, Phys. Rev. **73**, 155 (1948).
[13] C. Patton, J. Appl. Phys. **39**, 3060 (1968).
[14] M. Diehl, J.-Y. Yu, J. Heath, G. Held, H. Doyle, S. Sun, and C. Murray, J. Phys. Chem. B **105**, 7913 (2001).
[15] P. Dutta, A. Manivannan, M. Seehra, N. Shah, and G. Huffman, Phys. Rev. B **70**, 174428 (2004).
[16] Y. L. Raikher and V. I. Stepanov, Phys. Rev. B **50**, 6250 (1994).
[17] J. B. Youssef and C. Brosseau, Phys. Rev. B **74**, 214413 (2006).
[18] F. X. Redl, C. T. Black, G. C. Papaefthymiou, R. L. Sandstrom, M. Yin, H. Zeng, C. B. Murray, and S. P. O'Brien, J. Am. Chem. Soc. **126**, 14583 (2004).
[19] M. Yin, A. Willis, F. Redl, N. Turro, and S. O'Brien, J. Mater. Res. **19**, 1208 (2004).
[20] J. Hoshen and R. Kopelman, Phys. Rev. B **14**, 3438 (1976).
[21] Y. Guan and W. Bailey, J. Appl. Phys. **101**, D104 (2007).
[22] R. A. McCurrie, *Ferromagnetic Materials Structure and Properties* (Academic, New York, 1994), Vol. 4, p. 133.
[23] L. Brillouin, C. R. Hebd. Seances Acad. Sci. **194**, 255 (1932).
[24] C. Scheck, L. Cheng, I. Barsukov, Z. Frait, and W. Bailey, Phys. Rev. Lett. **98**, 117601 (2007).
[25] R. McMichael and P. Krivosik, IEEE Trans. Magn. **40**, 2 (2004).
[26] T. Ninjbadgar, T. Fukuda, and S. Yamamoto, Solid State Sci. **6**, 879 (2004).
[27] G. Bate and D. J. Craik, *Magnetic Oxides* (Wiley, London, 1975), p. 689.